Supporting Information

Rearrangement from the Heteroantiaromatic Borole to the Heteroaromatic Azaborine Motif

Sunanda Biswas,[a] Cäcilia Maichle-Mössmer,[b] Holger F. Bettinger[a,*]

[a] *Institut für Organische Chemie, Universität Tübingen, Auf der Morgenstelle 18,72076 Tübingen, Germany*

[b] *Institut für Anorganische Chemie, Universität Tübingen, Auf der Morgenstelle 18,72076 Tübingen, Germany*

Email: holger.bettinger@uni-tuebingen.de

Contents

General Procedures. All reactions and product manipulations were performed under argon atmosphere using Schlenk line technique or in an M-Braun glovebox. Dry *n*-hexane was collected from an M-Braun solvent purification system (SPS) just before use. All NMR spectra were recorded on Bruker DRX 250 MHz (^{11}B, ^{29}Si), 400 and AMX 600 MHz spectrometers (^{1}H, ^{13}C). The variable temperature ^{11}B NMR spectra were recorded on a Bruker AVANCE II+ 500 MHz operating at 160 MHz (^{11}B). The spectra were referenced to residual solvents (^{1}H, ^{13}C) or externally [^{11}B: BF_3•OEt_2, ^{29}Si: $Si(CH_3)_4$]. The NMR spectra were measured in CD_2Cl_2 or C_6D_6 that were purchased from Deutero GmbH. The N,O-bis(trimethylsilyl)hydroxylamine was purchased from Acros and used as received. The 9-chloro-9-borafluorene was synthesized according to the procedure reported previously.[1]

Synthesis of 6b. The bright yellow 9-chloro-9-borafluorene (80 mg, 0.403 mmol) was dissolved in 10 mL of *n*-hexane in a Schlenk tube and brought to –78 °C. Then 0.088 mL (0.411 mmol, 1.02 equivalents) amine **8c** was slowly added to the chloride solution. Immediate formation of colorless solid was observed. After complete addition of amine the yellow color of the chloride solution disappeared completely and the reaction mixture turned into a thick white solid slurry. Then the mixture was allowed to come to the room temperature slowly. The precipitate started to dissolve above –20 °C and a clear colorless solution was obtained at room temperature. Colorless solid precipitation was observed within a week from the concentrated *n*-hexane reaction mixture at –18 °C. The solid was collected and quickly washed with 1 mL cold hexane for two times and dried under vacuum to get 78 mg compound (73 %).

^{1}H (600 MHz, CD_2Cl_2): δ = 8.33 (d, J_{HH} = 8.16 Hz, 1H), 8.28 (d, J_{HH} = 8.0 Hz, 1H), 8.07 (d, J_{HH} = 7.50 Hz, 1H), 7.67-7.69 (m, 1H), 7.46 (t, J_{HH} = 7.35 Hz, 1H), 7.35-7.33 (m, 1H), 7.15-7.12 (m, 1H), 7.1 (dd, J_{HH} = 8.07, 1.05 Hz, 1H), 6.48 (br, N–H), 0.36 (s, TMS, 9H) ppm.;

$^{13}C\{^1H\}$ (150.9 MHz, CD_2Cl_2): δ = 141.0, 140.6, 133.1, 131.1, 128.5, 126.3, 124.2, 122.4, 122.3 120.7, 118.8, 1.8 ppm, C directly attached to the boron was not detected; $^{11}B\{^1H\}$ (80.3 MHz, CD_2Cl_2): δ = 27.3 (s, $h_{1/2}$ = 239 Hz) ppm; $^{29}Si\{^1H\}$ (49.7 MHz, CD_2Cl_2): δ = 11.4 ppm; UV-Vis (in *n*-hexane) λ_{max} (log ε) = 223(4.786), 228(4.764), 249(4.505), 269(4.402), 298(4.133), 311(4.19), 324(4.181) nm. HRMS(EI) ($C_{15}H_{18}BNOSi$): m/z calcd. 267.125072, found. 267.12677.

Synthesis of 6f: Compound **6f** was prepared from 80 mg (0.403 mmol) 9-chloro-9-borafluorene by reacting with 2.03 equivalents of amine **8c** (0.818 mmol, 0.175 ml). The synthesis and work up procedure were same as described for compound **6b**. (Yield: 86 mg, 76%) ^1H (400 MHz, C_6D_6): δ = 8.16 (d, J_{HH} = 8.16 Hz, 1H), 8.12 (d, J_{HH} = 7.99 Hz, 1H), 7.43-7.40 (m, 1H), 7.35 (dd, J_{HH} = 7.38, 0.96 Hz, 1H), 7.18 (td, J_{HH} = 7.25 Hz, 0.88 Hz, 1H), 7.13-7.11 (m, 1H), 7.00-6.97 (m, 1H), 6.74 (s, br, 1H), 6.61-6.60 (m, 1H), 6.41 (s, br, 1H), 0.17 (s, 9H) ppm; ^{13}C (100.6 MHz, C_6D_6): δ = 140.4, 139.8, 130.6, 130.58, 128.5, 126.0, 124.4, 123.0, 122.4, 120.2, 118.5, –1.2 ppm, C directly attached to boron was not observed; $^{11}B\{^1H\}$ (80.3 MHz, C_6D_6): δ = 28.3 (s, $h_{½}$ = 296 Hz) ppm; $^{29}Si\{^1H\}$ (49.7 MHz, C_6D_6): δ = 25.5 ppm; UV-Vis (in *n*-hexane) λ_{max} (log ε) = 226(4.579), 250(4.287), 271(4.181), 298(3.877), 312(3.948), 325(3.949) nm; HRMS(EI) ($C_{15}H_{19}BN_2OSi$): m/z calcd. 282.135971, found 282.13914.

Spectral data for compound 6b

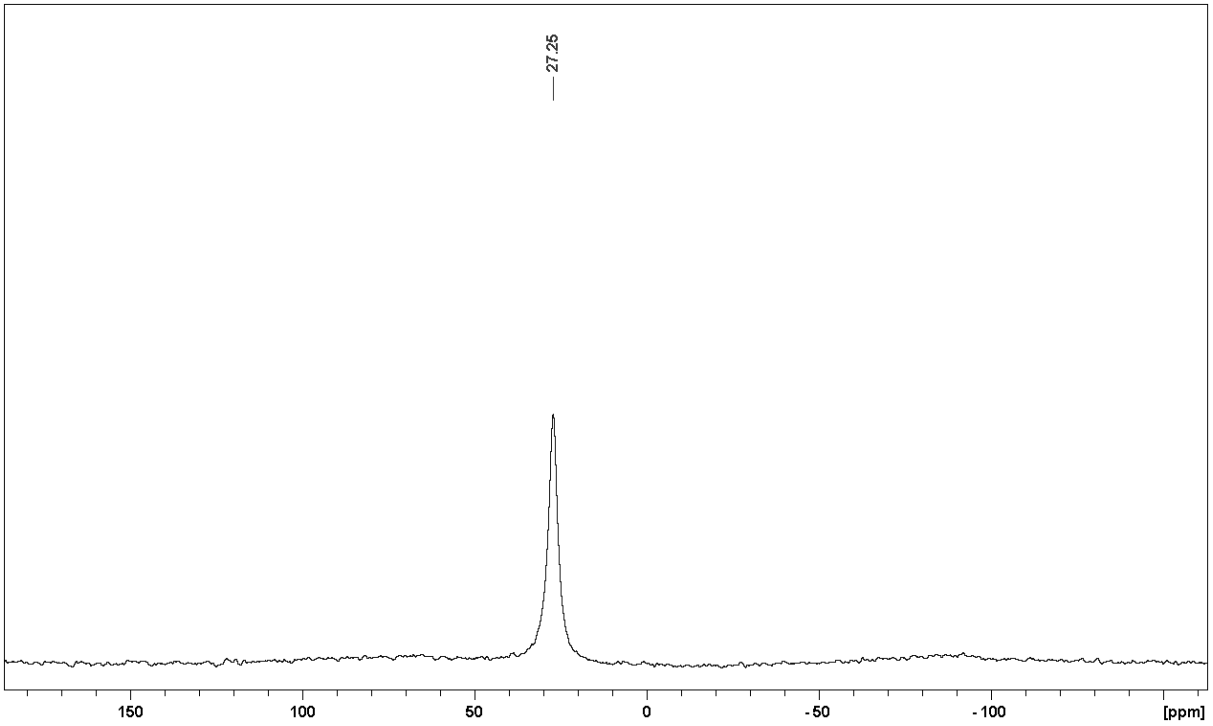

Figure S1. $^{11}B\{^{1}H\}$ NMR spectrum of **6b** in CD_2Cl_2 [$h_{½}$ = 239 Hz].

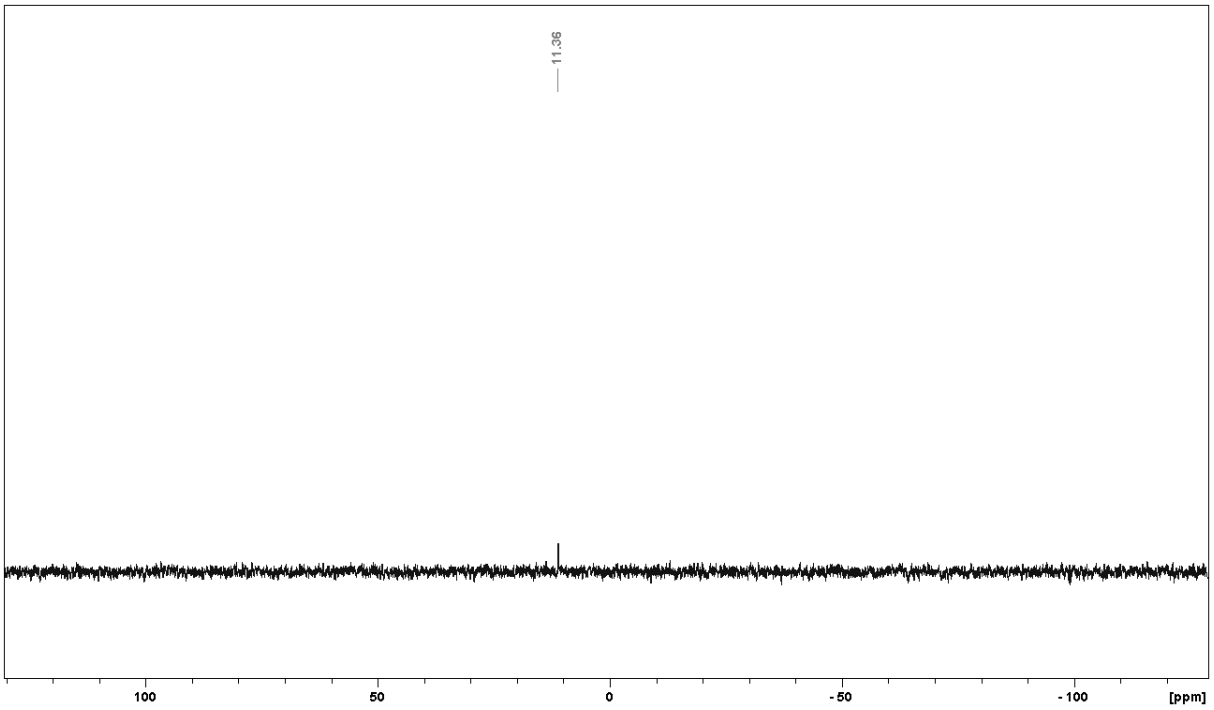

Figure S2. $^{29}Si\{^{1}H\}$ NMR spectrum of **6b** in CD_2Cl_2

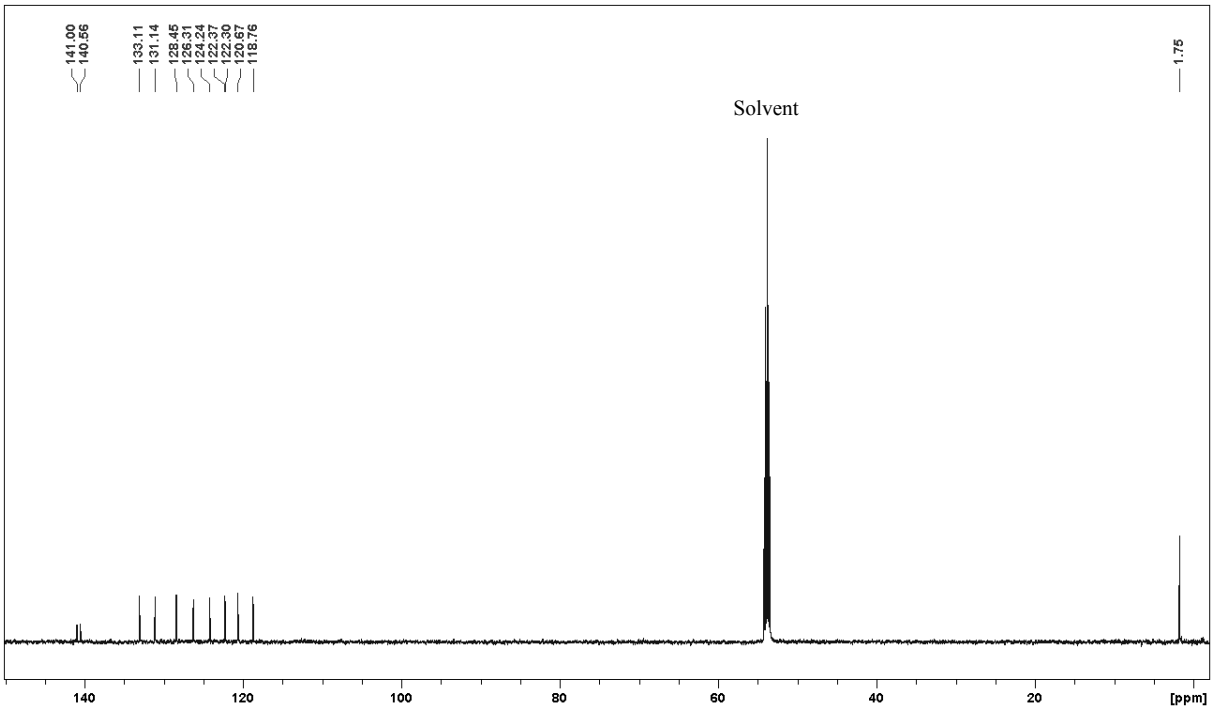

Figure S3. $^{13}C\{^{1}H\}$ NMR spectrum of **6b** in CD_2Cl_2.

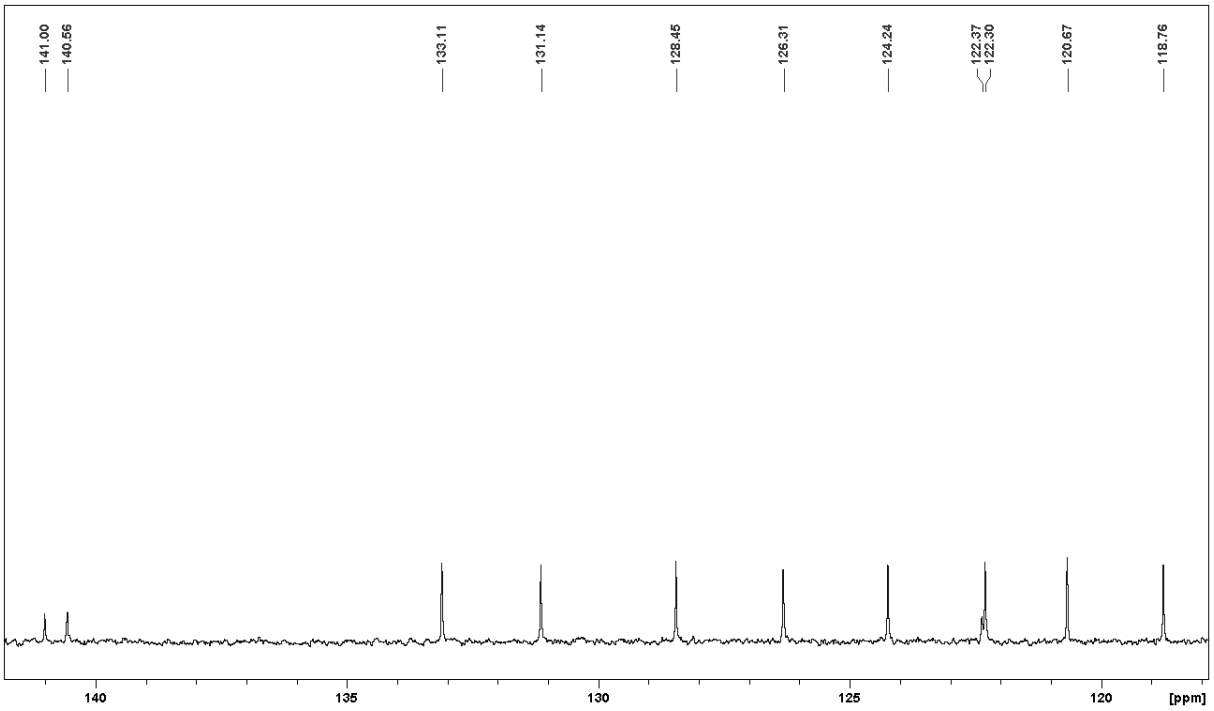

Figure S4. Extended view of aromatic region of $^{13}C\{^{1}H\}$ NMR spectrum of **6b**.

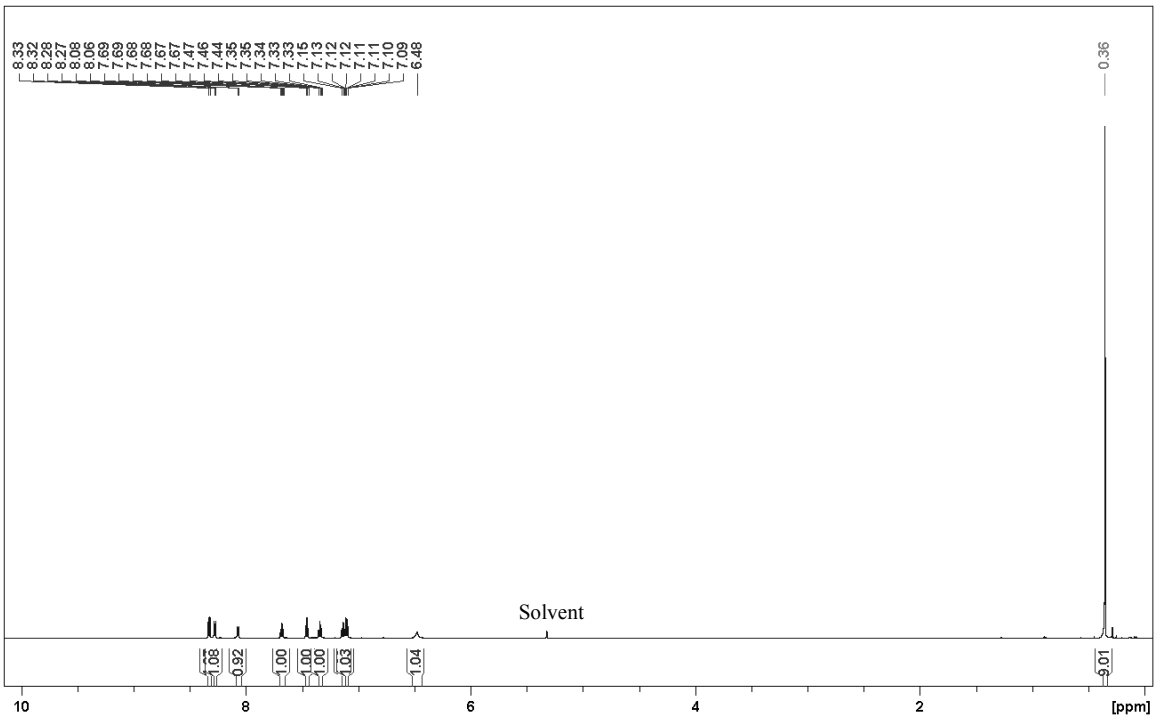

Figure S5. ^{1}H NMR spectrum of **6b** in CD_2Cl_2

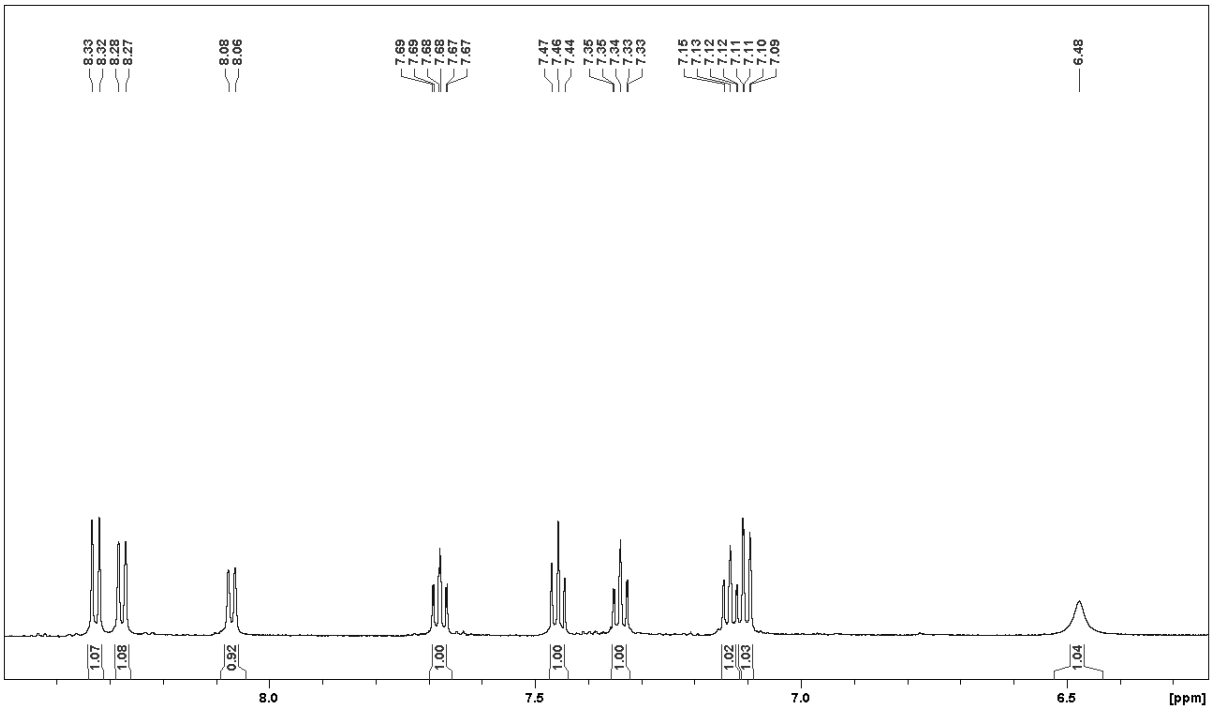

Figure S6. Extended view of aromatic region of ^{1}H NMR spectrum of **6b**.

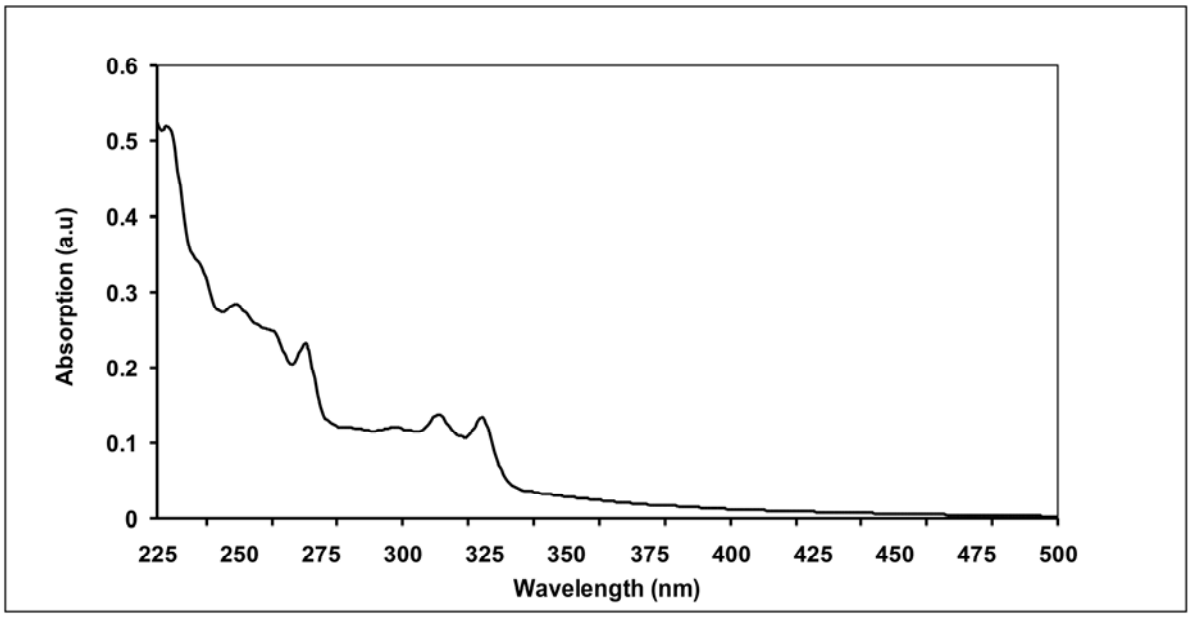

Figure S7. UV-Vis spectrum of **6b** in *n*-hexane

GC-MS:

Stationary Phase: J+W DB-5MS, 15 x 0.25 mm; d_f = 0.1 micron; temperature program = 80 °C (2 min) to 320 °C; temperature increasing rate = 6 °C/min; injection temperature = 300 °C; split method; flow rate = 1.1 ml min^{-1}; mass '(EI) at 70 eV; mobile phase: Helium.

Compound **6b** in dichloromethane, R_t = 19.33 min

The derivatized product of **6d** with N,O-*bis*(trimethylsilyl)trifluoroacetamide (BSTFA), in dichloromethane, R_t = 19.39 min

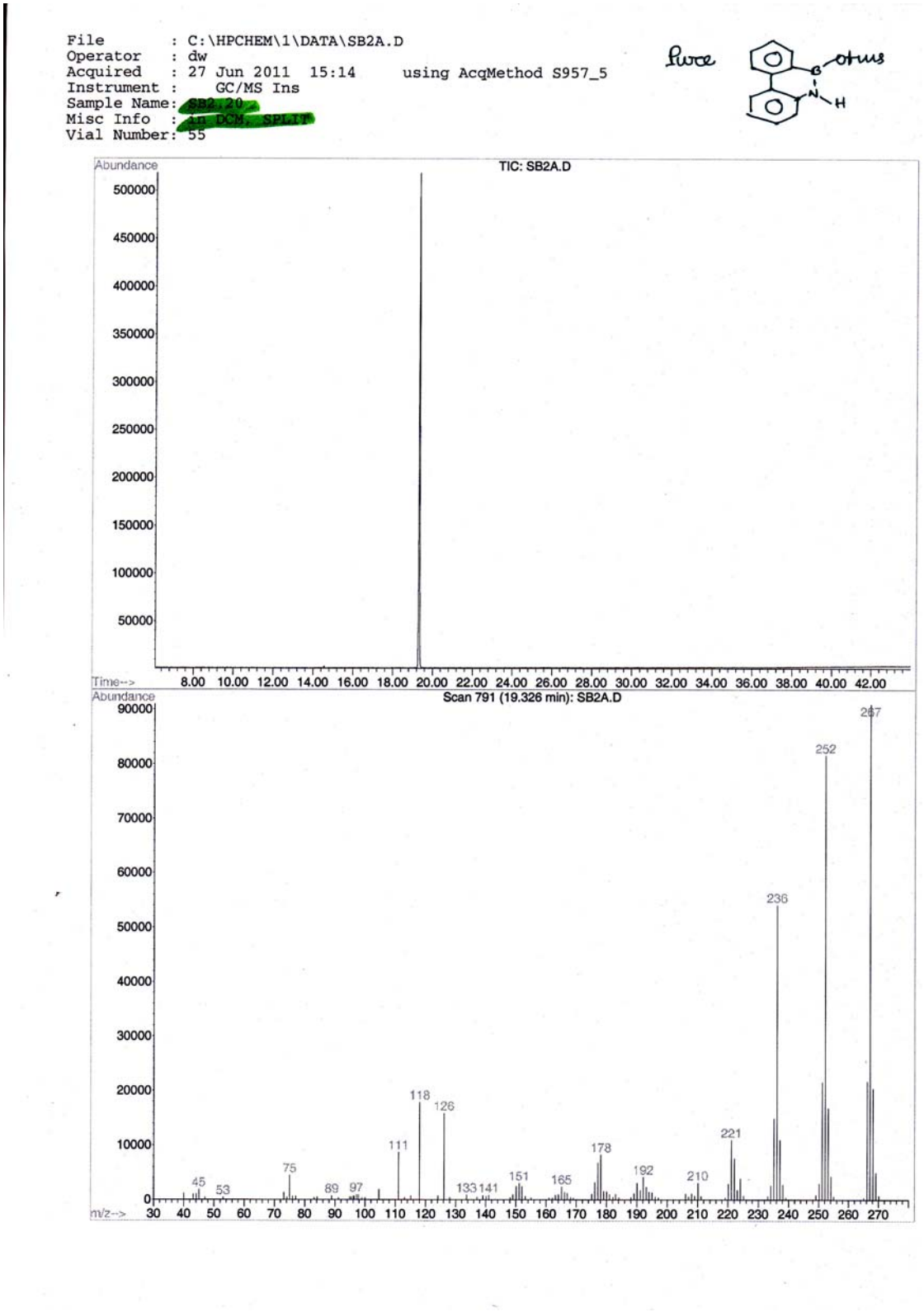

Figure S15. Gas chromatogram and corresponding mass spectrum of **6b**

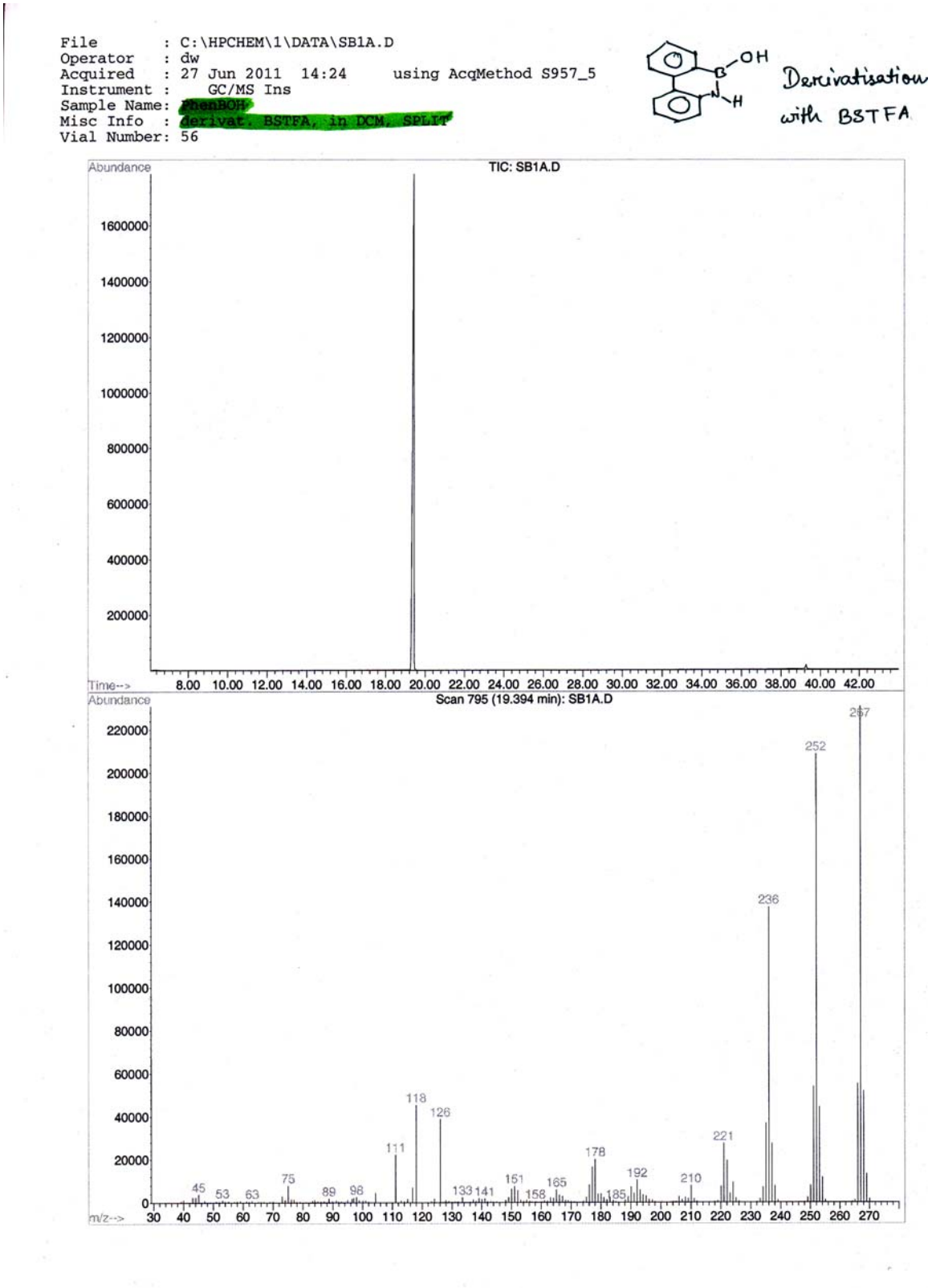

Figure S16. Gas chromatogram and corresponding mass spectrum of the derivatized product of **6d** with BSTFA.

Spectral data for compound 6f

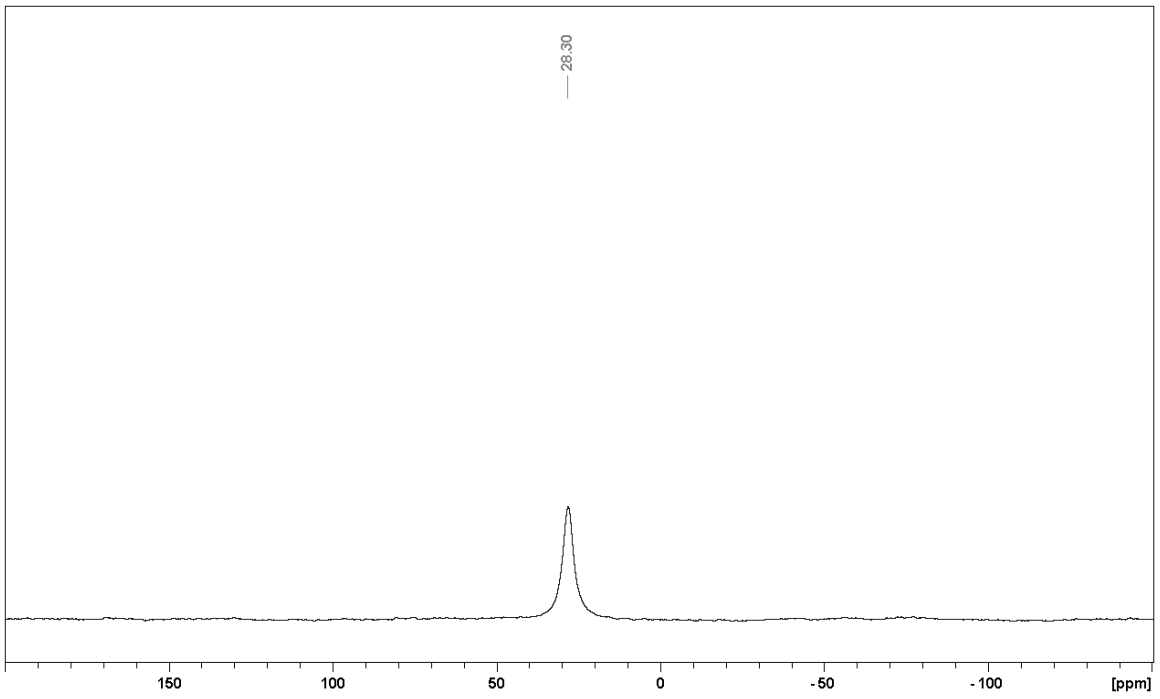

Figure S17. $^{11}B\{^{1}H\}$ NMR spectrum of **6f** in C_6D_6 [$h_{½}$ = 239 Hz].

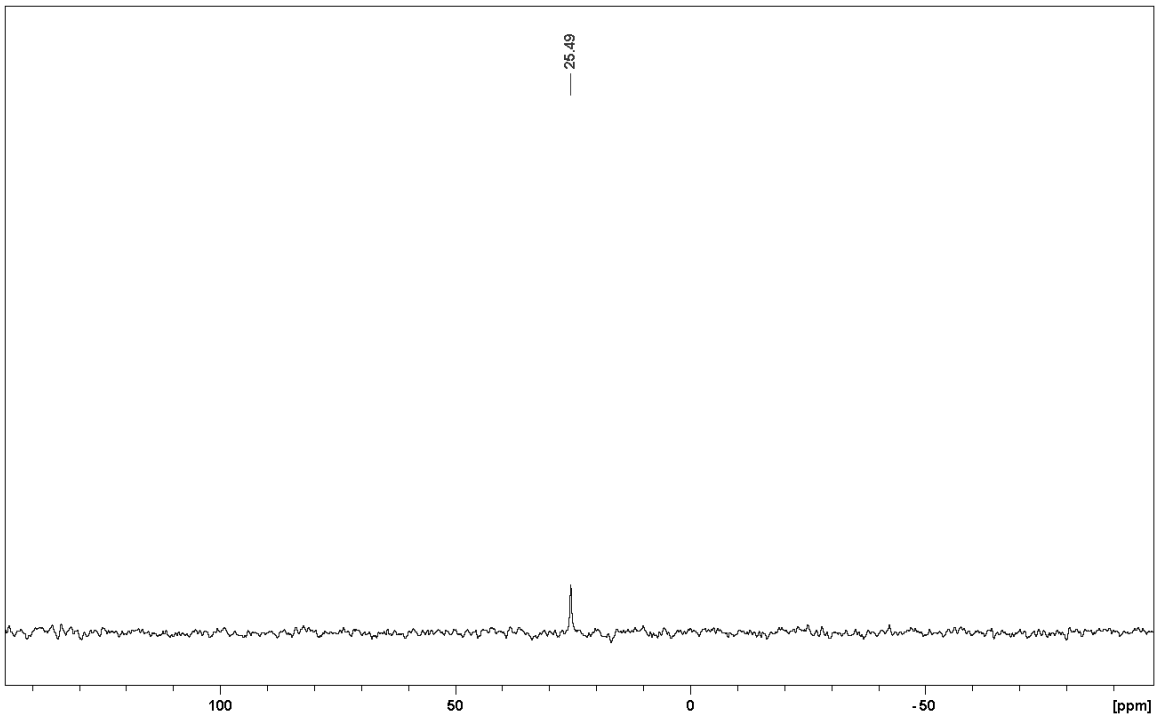

Figure S18. $^{29}Si\{^{1}H\}$ NMR spectrum of **6f** in C_6D_6.

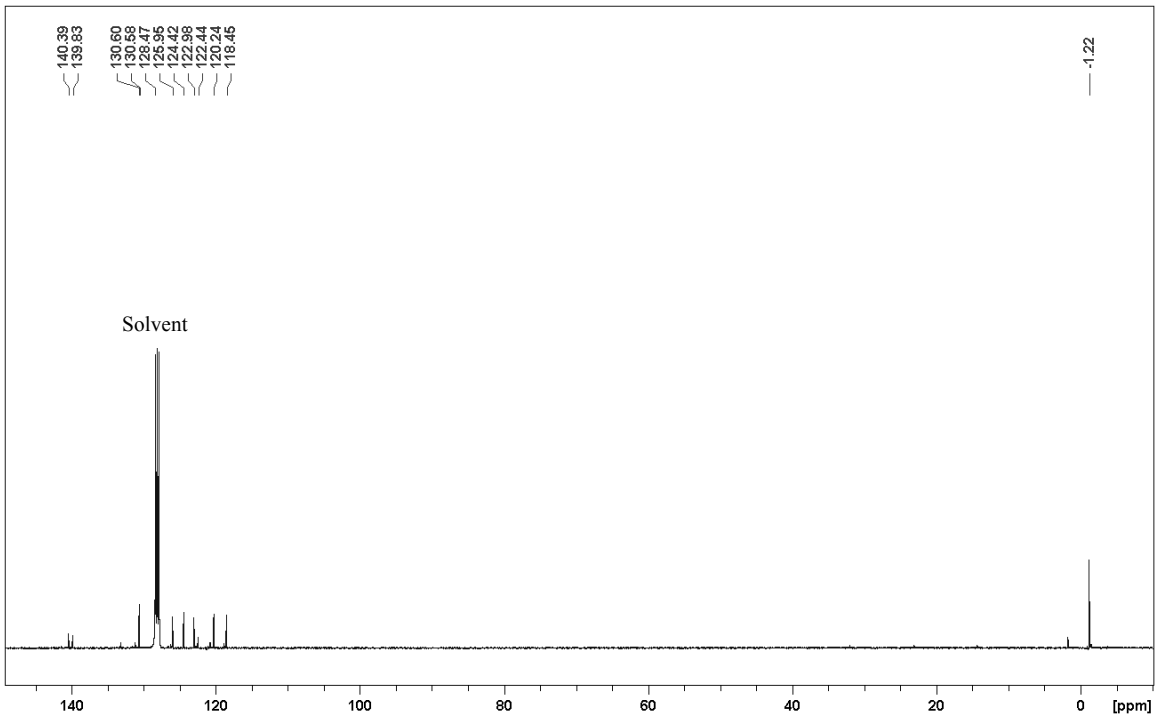

Figure S19. $^{13}C\{^{1}H\}$ NMR spectrum of **6f** in C_6D_6.

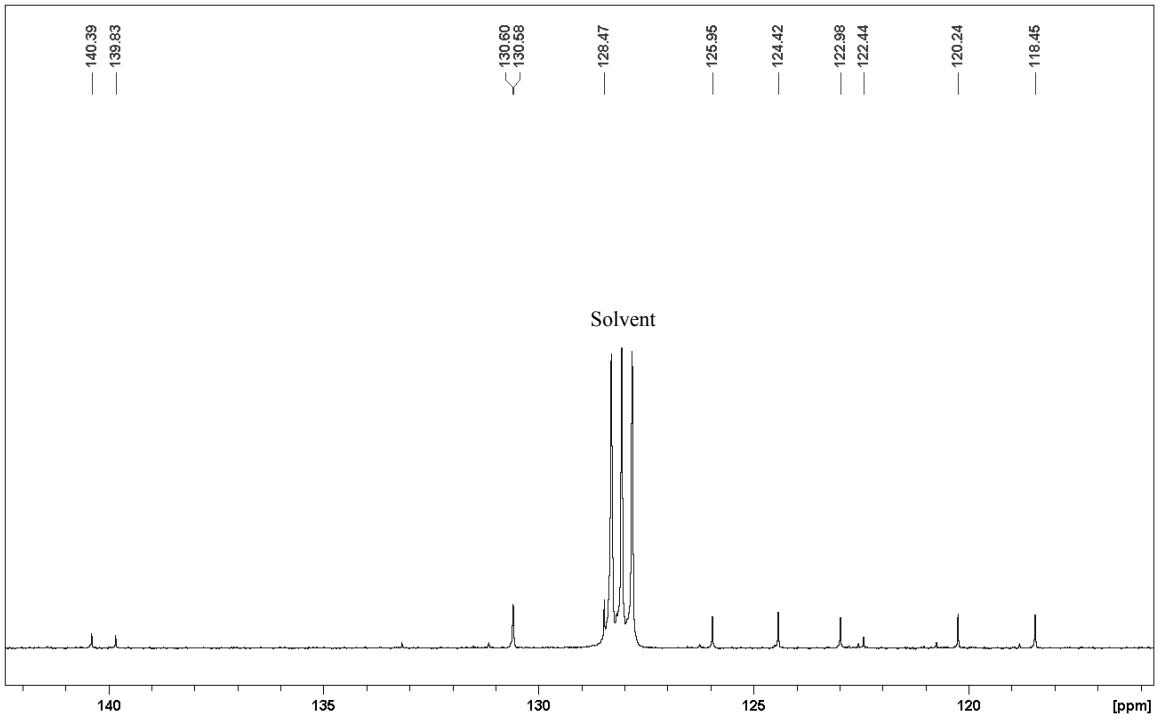

Figure S20. Extended view of the aromatic region of $^{13}C\{^{1}H\}$ NMR spectrum of **6f**.

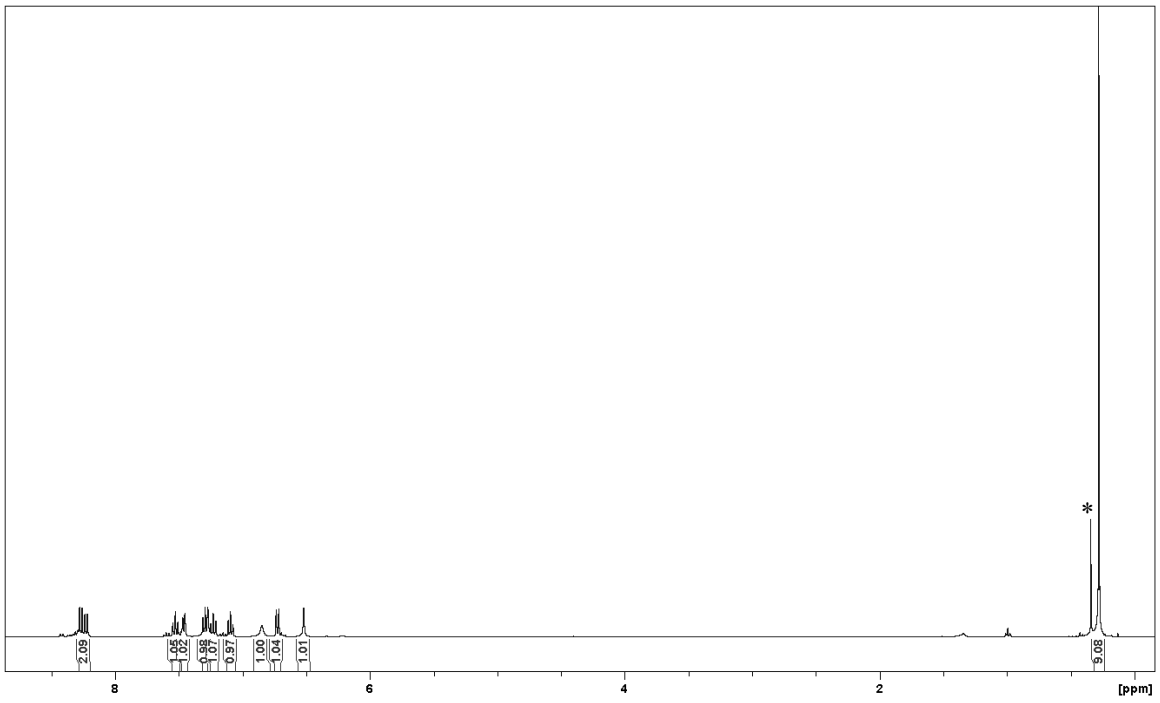

Figure S21. ^{1}H NMR spectrum of **6f** in C_6D_6.

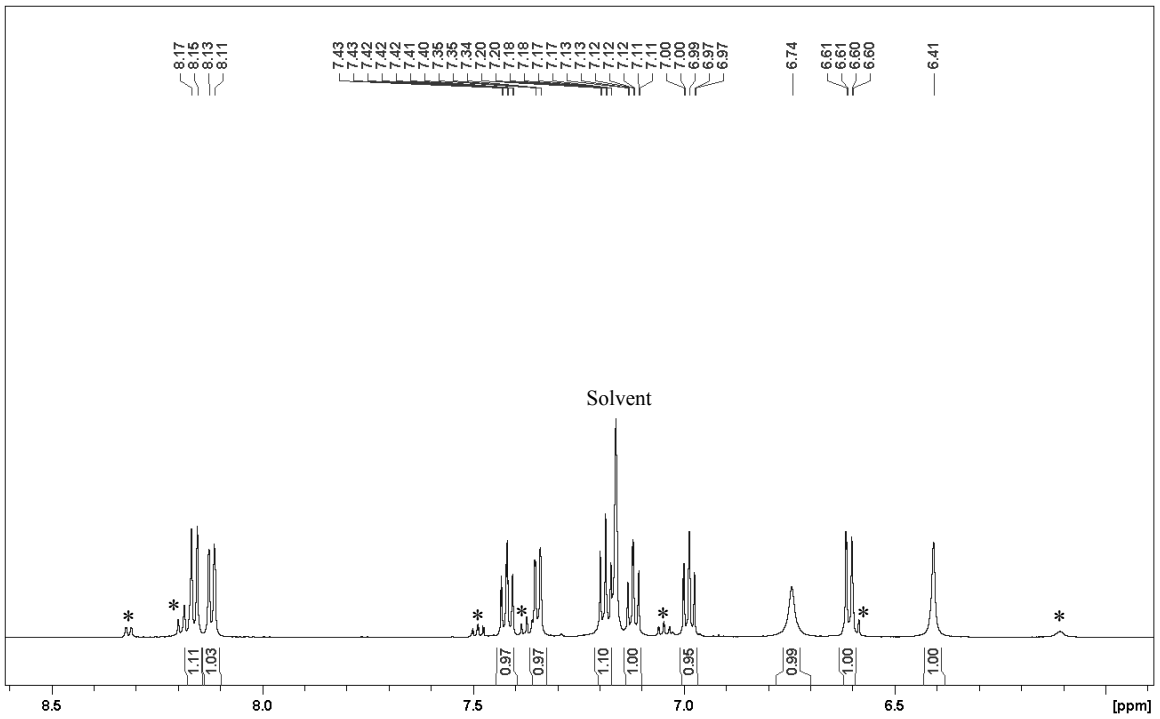

* Marked signals in **S21** and **S22** are due to **6b**

Figure S22. Extended view of the aromatic region of ^{1}H NMR spectrum of **6f**.

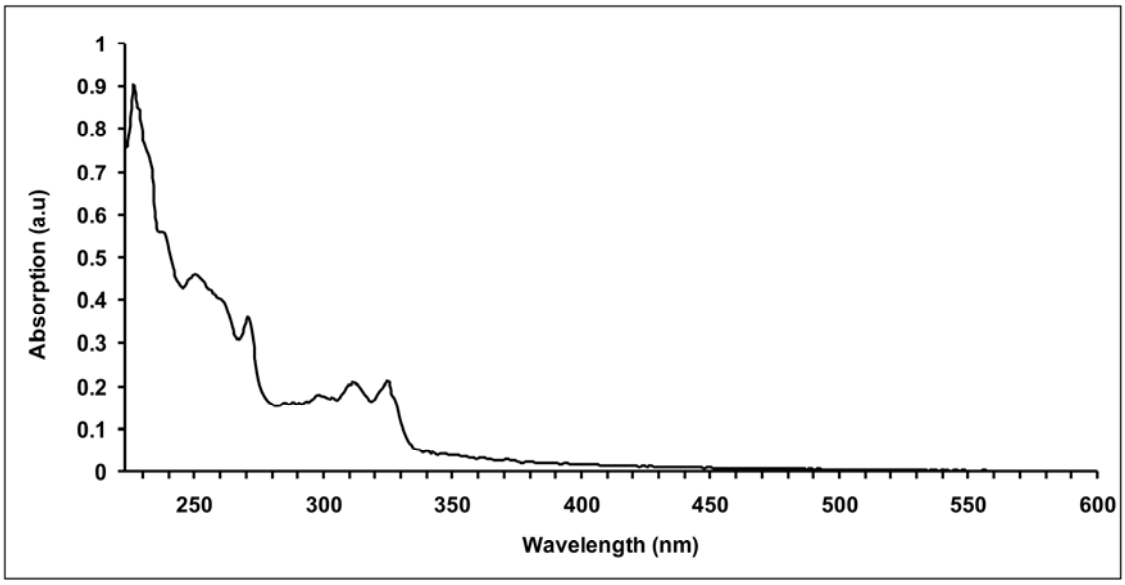

Figure S23. UV-Vis spectrum of **6f** in *n*-hexane.

X-ray Crystallographic Data for 6b

Table 1. Crystal data and structure refinement for $C_{15}H_{18}BNOSi$ (**6b**).

Empirical formula	$C_{15}H_{18}BNOSi$
Formula weight [g mol^{-1}]	267.20
Temperature [K]	173(2)
Wavelength [Å]	0.71073
Crystal system, space group	Monoclinic, $P2_1/n$
a [Å]	15.288(2)
b [Å]	5.8962(5)
c [Å]	16.276(2)
α [°]	90
β [°]	94.042(11)
γ [°]	90
Volume [Å^3]	1463.5(3)
Z	4
Calculated density [Mg/m^3]	1.213
Absorption coefficient [mm^{-1}]	0.151
F(000)	568
Crystal size [mm^3]	0.40 x 0.10 x 0.10
Theta range for data collection [°]	2.67 to 27.10
Limiting indices	$-19 \le h \le 19$, $-7 \le k \le 7$, $-20 \le l \le 20$
Reflections collected / unique	21898 / 3229 [$R_{(int)} = 0.0898$]
Completeness to theta = 27.10	99.9 %
Absorption correction	None
Refinement method	Full-matrix least-squares on F^2
Data / restraints / parameters	3229 / 0 / 244
Goodness-of-fit on F^2	1.233
Final R indices [I>2sigma(I)]	$R_1 = 0.0597$, $wR_2 = 0.1169$
R indices (all data)	$R_1 = 0.0751$, $wR_2 = 0.1231$
Largest diff. peak and hole [e.Å^{-3}]	0.335 and -0.261

Computational Details

The computational investigations employed spin-component scaled Møller-Plesset perturbation theory to second order within the resolution-of-the-identity approximation (SCS-RIMP2) for geometry optimization.[2, 3] All geometries were fully optimized using the def-SV(P) and def-TZVP basis set and the recommended fitting bases.[4-6] Second derivatives were computed at the SCS-RIMP2/def-SV(P) level of theory by numerical differentiation of analytic gradients to confirm that the structures correspond to minima and to arrive at zero point vibrational energies within the harmonic approximation. The energies given in the paper were determined at the SCS-RIMP2/def-TZVP level of theory and corrected for zero point vibrational energies that were obtained with the smaller def-SV(P) basis set.

Chemical shieldings were computed using the GIAO[7] approach and Becke's three parameter hybrid functional in conjunction with the correlation functional of Lee, Yang, and Parr (B3LYP)[8, 9] in conjunction with the def-TZVP basis set. The ^{11}B chemical shift on the BF_3•OEt_2 scale was obtained by reference to B_2H_6 and its experimental chemical shift ($\delta^{11}B$ = 16.6 ppm).[10] The Turbomole program was used for the SCS-RIMP2 and GIAO-B3LYP computations.[11, 12]

The dyotropic rearrangement was investigated using Becke's three parameter hybrid functional in conjunction with the correlation functional of Lee, Yang, and Parr (B3LYP)[8, 9] as well as the double hybrid method with an empirical dispersion correction (B2PLYPD)[13, 14] in conjunction with the 6-31G* basis set. All geometries were completely optimized and the nature of the stationary points as minima or saddle points was confirmed by analytic computation of second derivatives at both levels of theory. Exploratory computations were done at the more economic B3LYP/6-31G*; at this level of theory, also intrinsic reaction coordinates (IRC) were computed using the Hessian based predictor-corrector method.[15, 16] The IRC computations confirmed that the protonated transition state (displayed in Figure 3, right) connects to the protonated azaborine and the protonated borole derivatives. The neutral

transition state (displayed in Figure 3, left) also connects to the azaborine, but not directly to the borole derivative. Rather, an isomer (**A**) of the borole displayed below marks the end point of the IRC. Isomer **A** is characterized by an OTMS unit that is bridging the BN bond; it is 21 kcal mol^{-1} higher in energy than **5b** and 26 kcal mol^{-1} below the product forming transition state at the B3LYP/6-31G* level of theory. The formation of isomer **A** from **5b** was not investigated as it presumably is not the bottleneck for product formation. The transition states were then reoptimized at the B2PLYPD/6-31G* level of theory. The B3LYP and B2PLYPD calculations were performed with Gaussian 09.[17]

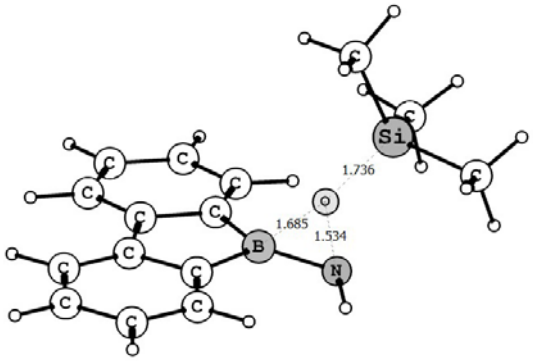

isomer A

References

1. S. Biswas, I. M. Oppel and H. F. Bettinger, *Inorg. Chem.*, 2010, **49**, 4499-4506.
2. S. Grimme, *J. Chem. Phys.*, 2003, **118**, 9095.
3. F. Weigend and M. Häser, *Theo. Chem. Acc.*, 1997, **97**, 331-340.
4. A. Schäfer, H. Horn and R. Ahlrichs, *J. Chem. Phys.*, 1992, **97**, 2571-2577.
5. A. Schäfer, C. Huber and R. Ahlrichs, *J. Chem. Phys.*, 1994, **100**, 5829-5835.
6. F. Weigend, M. Häser, H. Patzelt and R. Ahlrichs, *Chem. Phys. Lett.*, 1998, **294**, 143-152.
7. K. Wolinski, J. F. Hinton and P. Pulay, *J. Am. Chem. Soc.*, 1990, **112**, 8251-8260.
8. A. D. Becke, *J. Chem. Phys.*, 1993, **98**, 5648-5652.
9. C. Lee, W. Yang and R. G. Parr, *Phys. Rev. B*, 1988, **37**, 785-789.
10. B. Wrackmeyer, *Annu. Rep. NMR Spectosc.*, 1988, **20**, 61.
11. R. Ahlrichs, M. Bär, M. Häser, H. Horn and C. Kölmel, *Chem. Phys. Lett.*, 1989, **162**, 165-169.
12. TURBOMOLE V6.2 2010, a development of University of Karlsruhe and Forschungszentrum Karlsruhe GmbH, 1989-2007, TURBOMOLE GmbH, since 2007; available from http://www.turbomole.com.
13. S. Grimme, *J. Chem. Phys.*, 2006, **124**, 034108-034116.
14. T. Schwabe and S. Grimme, *Phys. Chem. Chem. Phys.*, 2007, **9**, 3397-3406.
15. H. P. Hratchian and H. B. Schlegel, *J. Chem. Phys.*, 2004, **120**, 9918-9924.
16. H. P. Hratchian and H. B. Schlegel, *J. Chem. Theory Comput.*, 2004, **1**, 61-69.
17. M. J. Frisch, G. W. Trucks, H. B. Schlegel, G. E. Scuseria, M. A. Robb, J. R. Cheeseman, G. Scalmani, V. Barone, B. Mennucci, G. A. Petersson, H. Nakatsuji, M. Caricato, X. Li, H. P. Hratchian, A. F. Izmaylov, J. Bloino, G. Zheng, J. L. Sonnenberg, M. Hada, M. Ehara, K. Toyota, R. Fukuda, J. Hasegawa, M. Ishida, T. Nakajima, Y. Honda, O. Kitao, H. Nakai, T. Vreven, J. A. Montgomery, J. E. Peralta, F. Ogliaro, M. Bearpark, J. J. Heyd, E. Brothers, K. N. Kudin, V. N. Staroverov, R. Kobayashi, J. Normand, K. Raghavachari, A. Rendell, J. C. Burant, S. S. Iyengar, J. Tomasi, M. Cossi, N. Rega, J. M. Millam, M. Klene, J. E. Knox, J. B. Cross, V. Bakken, C. Adamo, J. Jaramillo, R. Gomperts, R. E. Stratmann, O. Yazyev, A. J. Austin, R. Cammi, C. Pomelli, J. W. Ochterski, R. L. Martin, K. Morokuma, V. G. Zakrzewski, G. A. Voth, P. Salvador, J. J. Dannenberg, S. Dapprich, A. D. Daniels, Ö. Farkas, J. B. Foresman, J. V. Ortiz, J. Cioslowski and D. J. Fox, Gaussian, Inc., Wallingford CT, 2009.